Evidence of Transition-Metal Accumulation on Aged Graphite Anodes by SIMS

D. P. Abraham,[a,*,z] T. Spila,[b] M. M. Furczon,[a] and E. Sammann[b]

[a]*Argonne National Laboratory, Chemical Sciences and Engineering Division, Argonne, Illinois 60439, USA*
[b]*Frederick Seitz Materials Research Laboratory, University of Illinois at Urbana-Champaign, Urbana, Illinois 61801, USA*

In cells containing $Li_{1.05}(Ni_{1/3}Co_{1/3}Mn_{1/3})_{0.95}O_2$-based positive and graphite-based negative electrodes, a significant portion of cell impedance rise on aging is known to be from the negative electrode. One possible reason for this impedance rise is the dissolution of transition-metal elements from the oxide electrode that accumulate and create a high-impedance layer at the negative electrode–electrolyte interface. This article details dynamic secondary ion mass spectrometry (SIMS) measurements, which provide a relative comparison of Mn, Co, and Ni contents on fresh, formed, and aged graphite electrodes. The data clearly indicate that these transition-metal elements accumulate at the electrode surface and diffuse into the electrode during cell aging.
© 2008 The Electrochemical Society. [DOI: 10.1149/1.2987680] All rights reserved.

Research on alternative energy technologies for transportation applications has been stimulated by the rising costs of petroleum. At the present time hybrid electric vehicles (HEVs), which complement the internal combustion engine with a battery system, show promise for reducing petroleum consumption in automobiles. Battery systems based on lithium-ion technology are being extensively investigated for HEVs because of their higher energy storage and power densities.[1] Studies on lithium-ion battery materials and systems are being conducted at Argonne National Laboratory as part of the U.S. Department of Energy's Advanced Technology Development (ATD) program.[2-4] The goal of this program is to address key barriers (calendar life, safety concerns, high cell costs, and low-temperature performance) which have limited the successful commercialization of lithium-ion technologies for transportation applications.

Testing of the third generation of ATD cells (i.e., Gen3 cells) is currently in progress. Table I shows the chemistry of electrodes employed in these cells. The positive electrode active material is $Li_{1.05}(Ni_{1/3}Co_{1/3}Mn_{1/3})_{0.95}O_2$, whereas the negative electrode active material is mesocarbon microbead (MCMB)-10 graphite. The baseline electrolyte is 1.2 M $LiPF_6$ in 3 ethyl carbonate:7 ethyl methyl carbonate (by weight); most cells also contain 2–3 wt % $LiF_2BC_2O_4$ as an electrolyte additive, which appears to improve cell longevity. The Gen3 cells are being tested using both calendar (pulse-per-day) and cycle (continuous cycling) life profiles, with periodic interruptions for reference performance tests to gauge cell capacity and impedance changes as a function of aging. Data obtained in cells containing a Li–Sn reference electrode have indicated that a significant portion of the cell impedance rise can be attributed to the graphite negative electrode. This result is different from that of our Generation 2 cells, which contained $LiNi_{0.8}Co_{0.15}Al_{0.05}O_2(+)$ and Mag-10 graphite(−) electrodes, that showed only a small impedance rise at the negative electrode.[5]

The mechanisms that produce negative electrode impedance rise in Gen3 cells are yet to be conclusively identified. One hypothesis is that minute quantities of Mn dissolved from $Li_{1.05}(Ni_{1/3}Co_{1/3}Mn_{1/3})_{0.95}O_2$ migrate to the graphite anode and modify the solid electrolyte interphase (SEI) to produce a high-impedance layer; this mechanism is similar to that proposed for graphite impedance rise in $LiMn_2O_4(+)//graphite(−)$ lithium-ion cells.[6,7] However, examination of graphite anodes from aged Gen3 cells by techniques such as X-ray photoelectron spectroscopy (XPS) and energy-dispersive spectroscopy (EDS) show no detectable quantities of Mn.[8] These data suggest that either (*i*) Mn does not precipitate at graphite anodes during cell aging or (*ii*) Mn quantities at the

electrode are below the detection limits (~ 1000 ppm) of XPS and EDS instrumentation.

Secondary ion mass spectrometry (SIMS) is an ideal technique to determine trace levels of transition metals on graphite samples because of its excellent detection limits (ppb to ppm) and good depth resolution.[9] In dynamic SIMS, the sample is placed in vacuum and bombarded with a narrow beam of ions, called primary ions, which are sufficiently energetic to cause ejection of atoms and atom clusters from the sample. Some of these atoms and atom clusters are ejected as ions, called secondary ions. These ions are subsequently accelerated into a mass spectrometer, where they are separated and counted based on their mass-to-charge ratio. Elemental depth profiles of the sample can be obtained as a function of sputtering depth; the depth probed depends on the sample-layer sputtering rates and data-collection times.

In this article we describe the examination of fresh, formed, and aged Gen3 graphite electrodes by dynamic SIMS. The fresh electrodes were examined in the as-received condition, i.e., they were never in a lithium-ion cell. The formed electrodes were from Gen3 cells that were cycled three times between 3 and 4.1 V at 30°C. The aged electrodes were from Gen3 cells that were aged at 4 V and 55°C for 38 weeks before cell disassembly. These cells contained a Li–Sn reference electrode, which showed that the graphite electrode impedance rise was the main contributor to cell impedance rise. Both formed and aged cells contained the $LiF_2BC_2O_4$ electrolyte additive, which was 3% of the electrolyte weight. Cell disassembly and graphite electrode harvesting were conducted in an Ar-atmosphere glove box (<1 ppm H_2O, <5 ppm O_2). To wash off excess electrolyte residue, the formed and aged electrodes were soaked in dimethyl carbonate (DMC) for 30 min. The wash solvent was then replaced with fresh DMC and the samples soaked for another 30 min before being dried for SIMS examination.

The dynamic SIMS experiments were conducted on a Cameca IMS-5F system using a 12 kV O_2^+ primary ion beam with a beam current of 20 nA. Positive secondary ions were detected. Depth profiles were obtained with a raster size of 500×500 μm and an image field of 150 μm, and each species was analyzed for 1 s before switching to the next one. As shown in Table I, the electrodes contained ~ 10 μm graphite, vapor grown carbon fibers (VGCF), and

Table I. Gen3 cell electrode chemistry.

Positive electrode	Negative electrode
84 wt % $Li_{1.05}(Ni_{1/3}Co_{1/3}Mn_{1/3})_{0.95}O_2$	90 wt % MCMB 10-28
8 wt % PVdF binder (KF7208)	8 wt % PVdF binder (KF1100)
8 wt % SuperP carbons	2 wt % VGCF
58 μm thick composite coating	52 μm thick composite coating
20 μm thick Al current collector	18 μm thick Cu current collector
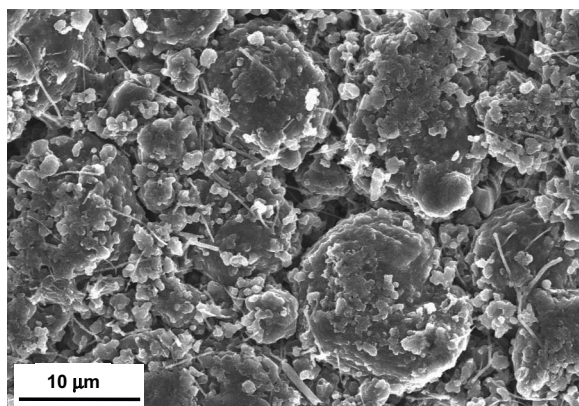
Figure 1. Scanning electron microscopy image of Gen3 negative electrode containing 90 wt % graphite, 2 wt % carbon fibers, and 8 wt % PVdF binder.

poly (vinylidene fluoride) (PVdF) binder (see Fig. 1). The data from each sample may, therefore, be considered as an average over the electrode surface. The samples were exposed to air for a few minutes before insertion into the SIMS chamber. This air exposure is not expected to alter the transition-metal content and distribution in the samples.

Figure 2 shows the C, Mn, Co, and Ni content of fresh, formed, and aged Gen3 graphite anodes as a function of sputter depth. For the fresh electrode, the highest counts are from carbon, which is as expected. The carbon counts are higher during the initial ∼150 s of sputtering and then level off, yielding ∼1000 counts per second (cps). The steady state-value is representative of the electrode matrix. The higher initial counts may be (*i*) associated with adventitious hydrocarbons adsorbed on the graphite surface that happen to ionize readily or (*ii*) related to the fact that it is easier to get C to ionize before the material gets fully churned up in the sputtering process, i.e., it is an artifact of the process that generates the secondary ions. The steady-state values for Mn and Co counts are ∼30 cps, whereas that for Ni is <10 cps; these data indicate trace levels of these elements in the electrode.

For the formed electrode also, the highest counts are from carbon; the steady-state C value is again ∼1000 cps. The steady-state values for Mn, Co, and Ni are ∼130, 100, and 20 cps, which are higher than those measured for the fresh sample; these higher counts may reflect either leaching of these elements from the oxide during cell formation or enhanced ionization of these elements induced by components, such as F, in the electrolyte residue. For the aged electrode, however, the maximum Mn cps are more than 2 orders greater

and the Co and Ni cps are more than an order of magnitude greater than for the formed sample. The data are clear evidence for the accumulation of these transition-metal elements on and in the negative electrode during cell aging. The initial dip in the C data corresponds to peaks in the Mn, Co, and Ni data.

The Fig. 2 data are replotted in Fig. 3 to highlight differences for individual elements in the various electrodes. It is clear that the Mn, Co, and Ni contents of the aged sample are significantly greater than those of the formed sample, especially at the electrode surface. The increase in transition-metal counts and decrease in C signal during the initial sputtering period may be an artifact of the sputtering process. As indicated earlier, the count rate in dynamic SIMS is heavily dependent upon the ionization efficiency, which depends upon the surface composition and structure. Large electric dipoles on the surface tend to yield large ionization efficiencies. The O_2^+ primary ion beam creates such dipoles when it impinges on the sample surface; these ions are simultaneously deposited on the surface by the primary beam and removed by sputtering. The increasing Mn, Co, and Ni count rates during the initial phase of sputtering may, therefore, be representative of the time taken for the near-surface oxygen concentrations to reach equilibrium. Alternatively, the data may indicate a subsurface enrichment of transition metals, buried under an overlying C-rich SEI layer.

The time required for the C data to reach a steady-state value is greater for the aged sample than for the formed samples. This feature could be due to a thicker SEI film or to a film that sputters slower on the negative electrode surface. In either case, the data indicate that the electrode surface film is different on the aged sample than on the formed sample. These differences, which may include changes in the morphology, constitution, and thickness of the surface film, correlate with the increase in negative electrode impedance induced by the cell aging process.

Although the SIMS data for the aged sample indicate a significantly higher cps value for Mn than for Co and Ni, we cannot directly conclude that the Mn concentrations are higher than those for Co and Ni because of differing ionization efficiencies for the various elements. Experiments are underway to correlate the SIMS data to actual transition-metal concentration levels in the samples. Studies to examine other elements, such as B, F, O, and P, are also in progress to fully delineate changes to surface films that may help explain the electrode capacity and impedance changes observed during cell aging.

Acknowledgments
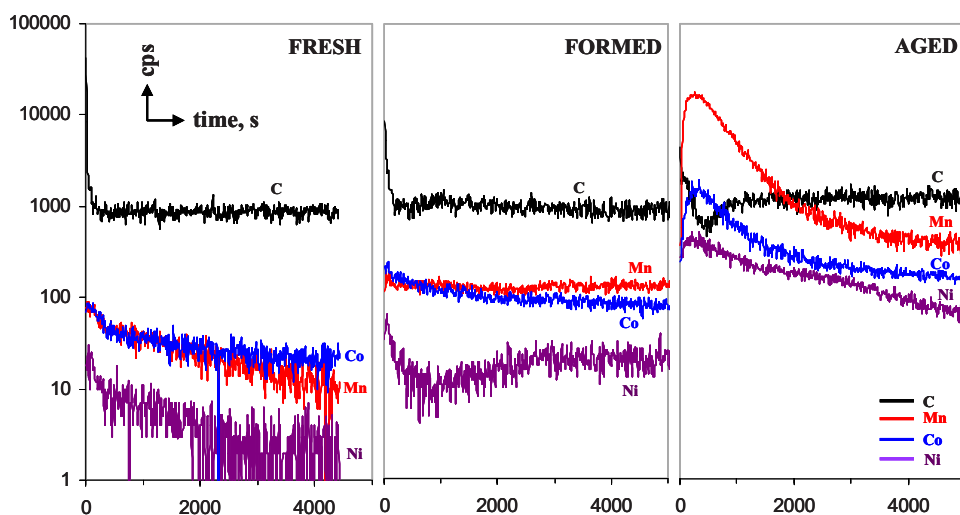
Figure 2. (Color online) Elemental content data as a function of sputter depth in fresh, formed, and aged Gen3 graphite anodes. The *X* axis shows sputtering time in seconds, and the *Y* axis shows counts per second.
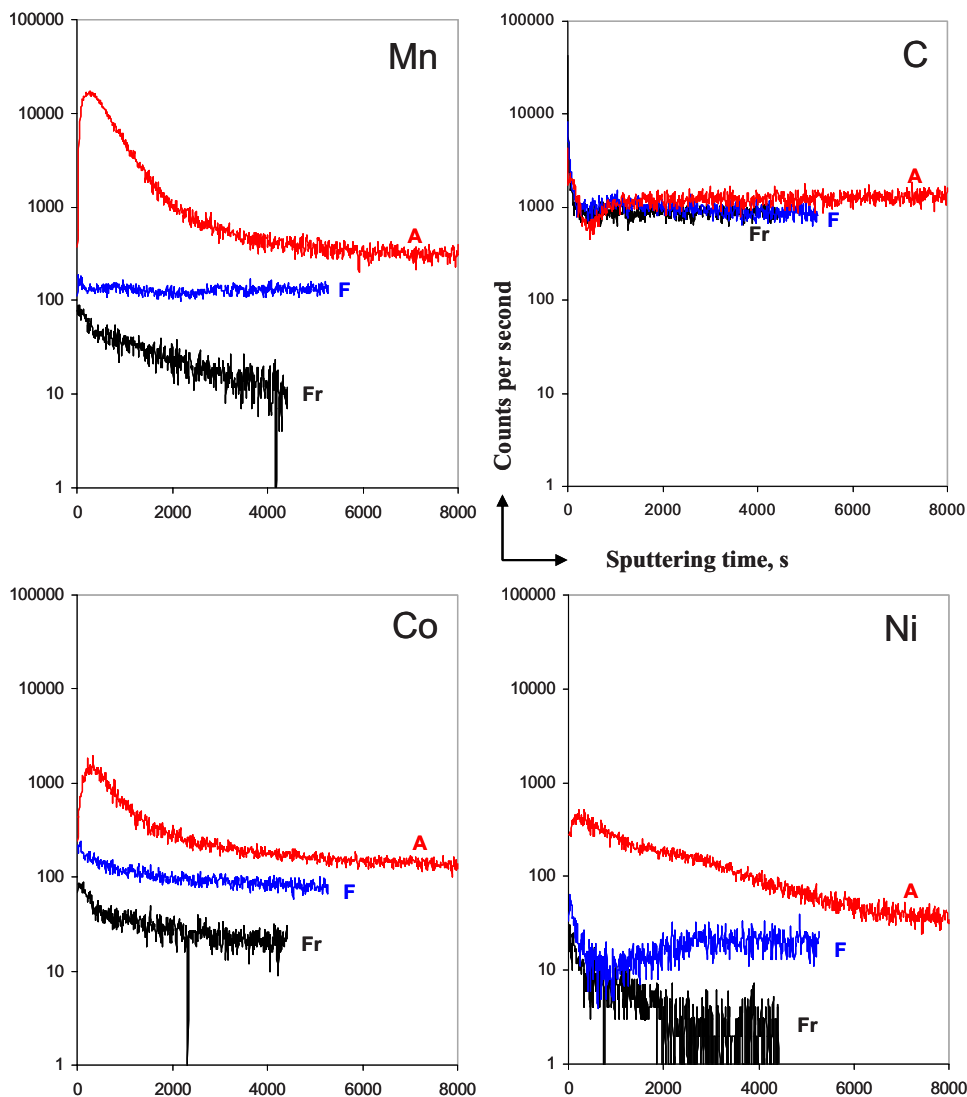
Figure 3. (Color online) Data in Fig. 2 replotted to show variations in Mn, Co, Ni, and C content in the fresh (Fr), formed (F), and aged (A) graphite anodes. The aged electrode shows the highest transition-metal content.

References

1. M. Armand and J.-M. Tarascon, *Nature (London)*, **451**, 652 (2008).
2. C. H. Lei, J. Bareño, J. G. Wen, I. Petrov, S.-H. Kang, and D. P. Abraham, *J. Power Sources*, **178**, 422 (2008).
3. D. P. Abraham, S. Kawauchi, and D. W. Dees, *Electrochim. Acta*, **53**, 2121 (2008).
4. D. P. Abraham, J. R. Heaton, S.-H. Kang, D. W. Dees, and A. N. Jansen, *J. Electrochem. Soc.*, **155**, A41 (2008).
5. D. P. Abraham, J. L. Knuth, D. W. Dees, I. Bloom, and J. P. Christophersen, *J. Power Sources*, **170**, 465 (2007).
6. D. H. Jang, Y. J. Shin, and S. M. Oh, *J. Electrochem. Soc.*, **143**, 2204 (1996).
7. A. Blyr, C. Sigala, G. Amatucci, D. Guyomard, Y. Chabre, and J.-M. Tarascon, *J. Electrochem. Soc.*, **145**, 194 (1998).
8. D. P. Abraham, Unpublished data (2008).
9. C. R. Brundle, C. A. Evans, Jr., and S. Wilson, Editors, *Encyclopedia of Materials Characterization*, Butterworth-Heinemann, Woburn, MA (1992).